ORIGINAL ARTICLE

Journal of Cachexia, Sarcopenia and Muscle 2023; **14**: 1737–1752
Published online 22 May 2023 in Wiley Online Library (wileyonlinelibrary.com) **DOI:** 10.1002/jcsm.13253

Slo1 deficiency impaired skeletal muscle regeneration and slow-twitch fibre formation

Chao Xia[1], Yonghui Wang[1], Tianyuan Jiang[2], Yan Hu[1], Yang Chen[2], Xinrun Ma[2], Xuemei Zhang[3]* & Yanhong Gao[1,2]*

[1]*Department of Geriatrics, Xinhua Hospital Affiliated to Shanghai Jiao Tong University School of Medicine, Shanghai, China;* [2]*Department of Geriatrics, Shanghai General Hospital Affiliated to Shanghai Jiao Tong University School of Medicine, Shanghai, China;* [3]*Department of Pharmacology, School of Pharmacy, Fudan University, Shanghai, China*

Abstract

Background It has been observed that Slo1 knockout mice have reduced motor function, and people with certain Slo1 mutations have movement problems, but there is no answer whether the movement disorder is caused by the loss of Slo1 in the nervous system, or skeletal muscle, or both. Here, to ascertain in which tissues Slo1 functions to regulate motor function and offer deeper insight in treating related movement disorder, we generated skeletal muscle-specific Slo1 knockout mice, studied the functional changes in Slo1-deficient skeletal muscle and explored the underlying mechanism.

Methods We used skeletal muscle-specific Slo1 knockout mice (Myf5-Cre; $Slo1^{flox/flox}$ mice, called CKO) as in vivo models to examine the role of Slo1 in muscle growth and muscle regeneration. The forelimb grip strength test was used to assess skeletal muscle function and treadmill exhaustion test was used to test whole-body endurance. Mouse primary myoblasts derived from CKO (myoblast/CKO) mice were used to extend the findings to in vitro effects on myoblast differentiation and fusion. Quantitative real-time PCR, western blot and immunofluorescence approaches were used to analyse Slo1 expression during myoblast differentiation and muscle regeneration. To investigate the involvement of genes in the regulation of muscle dysfunction induced by Slo1 deletion, RNA-seq analysis was performed in primary myoblasts. Immunoprecipitation and mass spectrometry were used to identify the protein interacting with Slo1. A dual-luciferase reporter assay was used to identify whether Slo1 deletion affects NFAT activity.

Results We found that the body weight and size of CKO mice were not significantly different from those of $Slo1^{flox/flox}$ mice (called WT). Deficiency of Slo1 in muscles leads to reduced endurance (~30% reduction, $P < 0.05$) and strength (~30% reduction, $P < 0.001$). Although there was no difference in the general morphology of the muscles, electron microscopy revealed a considerable reduction in the content of mitochondria in the soleus muscle (~40% reduction, $P < 0.01$). We found that Slo1 was expressed mainly on the cell membrane and showed higher expression in slow-twitch fibres. Slo1 protein expression is progressively reduced during muscle postnatal development and regeneration after injury, and the expression is strongly reduced during myoblast differentiation. Slo1 deletion impaired myoblast differentiation and slow-twitch fibre formation. Mechanistically, RNA-seq analysis showed that Slo1 influences the expression of genes related to myogenic differentiation and slow-twitch fibre formation. Slo1 interacts with FAK to influence myogenic differentiation, and Slo1 deletion diminishes NFAT activity.

Conclusions Our data reveal that Slo1 deficiency impaired skeletal muscle regeneration and slow-twitch fibre formation.

Keywords Slo1; Skeletal muscle; Myoblast; Myogenesis; Muscle regeneration; Slow-twitch fibre formation

Received: 9 October 2022; Revised: 3 April 2023; Accepted: 15 April 2023
**Correspondence to: Yanhong Gao, Department of Geriatrics, School of Medicine, Xinhua Hospital of Shanghai Jiaotong University, Shanghai 200092, China. Email: yanhonggao@sjtu.edu.cn*
Xuemei Zhang, Department of Pharmacology, School of Pharmacy, Fudan University, Shanghai, 201203, China. Email: xuemzhang@fudan.edu.cn
Chao Xia and Yonghui Wang contributed equally to this work.

Introduction

Skeletal muscle is made up of elongated multinuclear cells called myocytes (or myofibres), which are derived from myoblast fusion during prenatal development. Myoblasts have been shown to be capable of myogenic differentiation.[1] Adult skeletal muscle possesses amazing regeneration potential, mainly due to myoblasts, a population of muscle-resident stem cells. When myofibres are damaged, myoblasts proliferate and then differentiate and fuse into multinuclear myofibres, allowing damaged muscle to be repaired or replaced. Insulin-like growth factor 1 (IGF-1), Notch, Wnt, and interleukin-6 are just a few of the signalling pathways and molecules that have been reported to regulate myoblast fate regulation.[2–4] However, it is not completely clear what signalling affects myoblast function and how it modulates the state of myoblasts.

The primary function of the muscle is determined by the predominant fibre type in a muscle.[5] Mammalian skeletal muscle is made up of a variety of myofibres with different contraction speeds and metabolic qualities to accommodate a variety of motor activities. In general, slow-twitch (type I) myofibres contain many mitochondria and have high oxidative capacity and good endurance. Fast-twitch (type II) myofibres, on the other hand, have smaller mitochondria, use ATP predominantly through glycolysis, and contract relatively rapidly for short-term activity. However, muscle fibre types and these phenotypes are not perfectly aligned as once believed and myofibres are not fixed units and can change their phenotypic profile in response to functional demands. The molecular regulation of fibre type determination remains a mystery. Recent research has begun to pinpoint some of the factors that alter the distribution of fibre types. Calcineurin, AMP-activated protein kinase (AMPK), peroxisome proliferator-activated receptor gamma coactivator 1-alpha (PGC-1), and protein kinase C are all involved in the formation of oxidative myofibres.[6,7]

The Slo1 channel, also known as BK or MaxiK, differs from other K^+ channels in that it has an extremely large single-channel conductance and is regulated by both intracellular Ca^{2+} and membrane voltage.[8] The Slo1 channel serves as a hub in a variety of physiological processes that link membrane excitability to Ca^{2+} signalling events, such as neuronal excitability, muscular contraction, audition, hormone secretion, neurotransmitter release, and sleep duration.[9,10] Deficiencies in the Slo1 channel are associated with a spectrum of pathophysiological conditions including movement disorders, hypertension, epilepsy, intellectual disability, and autism.[11] The Slo1 channel is subjected to many mechanisms, including alternative splicing, auxiliary subunit modulation, posttranslational modifications, and protein–protein interactions.

Slo1, the α subunit of this channel forms the conducting pore and is encoded by a single gene, Slowpoke (KCNMA1). In addition to acting as the α subunit, the significance of Slo1 in cell signalling is becoming clearer as emerging evidence suggests Slo1 interacts with a variety of proteins not just at the plasma membrane but also in internal organelles. Many protein partners of Slo1 have been detected and confirmed, including β1-integrin, Akt, GSK-3β, PDK1, FAK, and Src.[12,13] Slo1 has been detected in both neurons and muscles in *C. elegans*, and evidence for its significance in motor function has been confirmed.[14,15] Furthermore, it has been observed that Slo1 knockout mice have reduced motor function,[16–19] and people with certain Slo1 mutations have movement problems, but there is no answer whether the movement disorder is caused by the loss of Slo1 in the nervous system, or skeletal muscle, or both. Given that other studies found Slo1 can affect myoblast differentiation in patients with hypokalaemic periodic paralysis and muscular dystrophy,[20,21] and mice with complete knockout of Slo1 showed a decrease in muscle mass and strength, we assumed that this phenomenon is caused, in part at least, by the deficiency of Slo1 in skeletal muscle. Therefore, we wanted to develop the mouse model by generating skeletal muscle-specific Slo1 knockout mice and to ascertain in which tissues Slo1 functions to regulate motor function and offer deeper insight in treating related movement disorder.

Here, we assess the role of Slo1 in the regulation of skeletal muscle phenotype and function. Although the slightly but significantly loss of strength has been observed, there is no obvious muscle atrophy in CKO mice. We show that Slo1 is mainly expressed in slow-twitch muscle fibres. Interestingly, Slo1 deletion in skeletal muscle impaired myoblast differentiation and slow-twitch fibre formation.

Methods

Animal experiments

All mice used in the experiments were maintained in the C57BL/6 background. Animal experiments of this study were approved by the Ethics Committee of Xinhua Hospital Affiliated to Shanghai Jiao Tong University School of Medicine.

The $Slo1^{flox/flox}$ mouse line, which has been described in our previously published study,[22] and Myf5-Cre (Jackson Laboratories) mice were crossed to generate skeletal muscle specific Slo1-deficient mice. The experiment was performed twice with independent cohorts.

To detect Slo1 protein expression during postnatal development, as the skeletal muscles were too small to be dissected completely in newborn mice, whole calf muscle complex was collected from WT mice at postnatal days 3, 5, 8, and 14 (three mice each group).

Given that the tibialis anterior (TA) is commonly used for regeneration studies, and as a result of its superficial position, TA was used as the damaged sites in $BaCl_2$-induced in-

jury model. In brief, 10-week-old WT and CKO mice were anaesthetised, legs were cleaned with alcohol, and tibialis anterior (TA) muscles were intramuscularly injected with 50 μL of 1.2% $BaCl_2$ (Sigma, USA) and harvested 3, 7, and 14 days after injury.

Exercise tolerance and forelimb grip strength test

Eight- to 12-week-old WT and CKO mice ran on the treadmill. Mice first ran at 10 m/min with 0% grade for 5 min, and the speed was increased by 2 m/min every 2 min until they were exhausted. The criterion of exhaustion was defined as the inability of the animal to run on the treadmill for 10 s despite mechanical prodding. Running time was calculated.

A force tension apparatus (grip strength meter, Bioseb) was used to measure forelimb grip strength. As a mouse grasped the bar, the peak pull force in grams was recorded on a digital force transducer. We conducted the procedure at a constant speed sufficiently slow to permit mice to build up a resistance against it and performed 6 consecutive measurements at one-minute intervals.

Cell culture

The isolation of primary myoblasts was conducted as the protocol described.[23] In brief, hind limb muscles was collected and dissected into small pieces followed by digestion with collagenase II (Worthington Biochemical, cat. no. 4176) in a shaking water bath at 37°C. Myoblasts were then isolated and maintained in F-10 culture medium containing 20% FBS, 1% penicillin, and 1% streptomycin. To obtain myotubes, myoblasts of 80% confluence were cultured in differentiation medium containing 2% horse serum for 3 days.

RNA extraction and quantitative real-time PCR

Total RNA extraction and quantitative real-time PCR method has already been described previously.[24] The fold change was calculated with the $2^{-\Delta\Delta CT}$ method and normalized to the level of the housekeeping gene GAPDH. The primer sequences used in this study are listed in Table S1.

RNA sequencing

Total RNA was isolated from cells using the RNeasy Mini Kit (QIAGEN, cat. no. 74104). Strand-specific cDNA libraries were generated using the Illumina TruSeq Stranded Total RNA Library Prep Kit with Ribo-Zero Gold. cDNA quality was determined using the Agilent high-sensitivity DNA kit on an Agilent 2100 BioAnalyzer (Agilent Technologies). Paired-end 125 BP reads were generated on an Illumina HiSeq 2500 instrument at the Oebiotech.corp. Reads were aligned to the GRCh38.p7 genome using TopHat v2.1.1 with the library type option set to first strand. Fragments per kilobase per millions (FPKMs) of known genes were calculated using express v1.5.1.

Gene set enrichment analysis

The gene expression dataset was transferred to the Gene Set Enrichment Analysis software (http://www.broadinstitute.org/gsea), and the analysis was carried out with default parameters except that the 'exclude smaller sets' was set to 25 and gene permutation was applied. We used a modified list of the C2 and C5 symbols gene set (http://www.broadinstitute.org/gsea/msigdb). FDR q-value < 0.25 was considered statistically significant.

Western blotting

Cells were lysed with cold RIPA buffer with protease and phosphatase inhibitors. Muscle tissues were lysed with the same buffer using stainless steel grinding balls. The concentration of the lysates was measured with the BCA protein assay kit (Thermo Scientific, cat. no.23225) following the manufacturer's instructions. The samples were loaded to SDS-polyacrylamide gel, proteins were transferred to PVDF membranes and incubated with primary antibody at 4°C overnight, and then further immunoblotted with HRP-conjugated antibody at 37°C for 1 h, developed with enhanced chemiluminescence (ECL) substrate (Millipore, cat. no. WBKLS0500) and chemiluminescence detection by ChemiDocTM MP Imaging System (Bio-Rad). Primary antibodies and dilutions used were as follows: MYH3 (cat. no. sc-53091), Pax7 (cat. no. sc-81648), MyoG (cat. no. sc-12732) (1:200, Santa Cruz Biotechnology); Slo1 (1:1000, Alomone Labs, cat. no. APC-021); HSC70 (cat. no. 8444), p70S6K (cat. no. 9202), p-p70S6K (cat. no. 97596), AKT (cat. no. 4691), p-AKT (cat. no. 4060) (1:1000, Cell Signaling Technology); BA-F8, BF-F3 (1:250, Developmental Studies Hybridoma Bank); GAPDH (cat. no. 60004-1-Ig), α-tubulin (cat. no. 11224-1-AP) (1:5000, Proeintech).

For immunoprecipitation of Slo1 and FAK, cell lysates were precleared with 5 μg of appropriate control IgG (Santa Cruz Biotechnology, cat. no. sc-2025) and 20 μL of protein A/G plus-agarose (Santa Cruz Biotechnology, cat. no. sc-2003) for 1 h rotation at 4°C. Lysates were centrifuged (500× g for 5 min at 4°C) and 5 μg of Slo1 (Alomone Labs) or FAK (Cell Signaling Technology, cat. no. 3285) antibody or corresponding IgG was added to the precleared lysates and kept on ice for 4 h. After incubation, 30 μL of protein A/G plus-agarose was added to each tube and kept on a rotator overnight at 4°C. Lysates were then centrifuged (500× g

for 5 min at 4°C). The pellet fractions were washed four times and then resuspended in 20 μL loading buffer. Samples were electrophoresed and immunoblotted with the appropriate antibody.

Histochemistry and immunofluorescence

Mouse muscle samples were frozen in liquid nitrogen-cooled isopentane in Tissue-Tek OCT. 10 mm sections were stained with haematoxylin–eosin staining and using the following primary antibodies: Slo1 (1:500, Alomone Labs), WGA (conjugated Alexa Fluor 488, Thermo Scientific, cat. no. W6748), and Desmin (1:1000, Abcam, cat. no. ab32362).

Primary mouse myoblasts were cultured in differentiation medium for 3 days and fixed with 4% paraformaldehyde for 15 min and stained with MYH3 (1:100, Santa Cruz Biotechnology) for myotubes.

For signal detection, Alexa Fluor 594-conjugated secondary antibodies (1:500, Biolegend, cat. no. 406709) were used. Nuclei were labelled with DAPI.

RNA interference

Small interfering RNA (siRNA) against mouse FAK, Slo1 and negative control were purchased from Shanghai Genechem Co., Ltd. (Shanghai, China). siRNA was transfected using Lipofectamine 2000 transfection reagent (Thermo Fisher Scientific, USA, cat. no. 11668019) according to the manufacturer's recommendations.

Luciferase reporter gene assay

Myoblasts were transfected with NFAT-luc (firefly luciferase plasmid; Yeasen, China, cat. no. 11512ES03) and pRL-TK (Renilla luciferase plasmid; Promega, USA, cat. no. E6881) using Lipofectamine 2000. TK-Renilla luciferase was used as a transfection control. Promega's dual luciferase assays were performed according to the manufacturer's instructions. All experiments were done in quadruplicate and repeated at least three times.

Statistical analysis

All data are expressed as the mean ± standard deviation (SD) and were analysed using GraphPad Prism 8 (GraphPad Software, Inc.). Differences between two groups were evaluated by unpaired two-tailed Student's t-test. Comparisons among three or more groups of independent samples were made with one-way ANOVA and Dunnett's test for multiple comparisons against the same control value. All experiments were performed at least three times, and $P < 0.05$ was considered statistically significant and the significance is indicated by $^{*}P < 0.05$, $^{**}P < 0.01$, and $^{***}P < 0.001$.

Results

The expression of Slo1 in skeletal muscles and myoblasts

Many other studies have shown the expression of Slo1 in skeletal muscle; however, expression of Slo1 differs depending on muscle phenotype. For instance, slow-twitch rat fibres indeed showed an elevated expression of Slo1. In contrast, Slo1 found in the fast-twitch rat fibres showed low expression.[25] In this study, we found that Slo1 was expressed mainly on the cell membrane (Figure 1A) and showed higher expression in soleus muscles (predominantly slow-twitch) than in gastrocnemius muscles (primarily fast type) (about 6.5-fold change, $P < 0.001$; Figure 1B).

We next investigated the in vivo expression of Slo1 during muscle postnatal development and muscular post-injury regeneration (Figure S1a, b). Slo1 protein expression was progressively reduced during muscle postnatal development (Figure 1C) and regeneration after injury (Figure 1D). To test the expression of Slo1 in myoblast differentiation in vitro, we isolated and studied primary mouse myoblasts. These cells can differentiate into myotubes with multiple nuclei and express MYH3, the myogenic marker at the later stage of myogenesis, thus displaying stem cell characteristics (Figure S1c, Figure 1E). We found that the expression of Slo1 was strongly reduced at the protein level during myoblast differentiation (Figure 1F, Figure S1d–f). All the above in vivo and in vitro studies suggest that Slo1 is associated with myogenesis.

Deficiency of Slo1 in muscles leads reduced endurance and strength

To investigate the role of Slo1 in skeletal muscle, we developed a specific knockout mouse. The generation process and identification of CKO mice are shown in Figure S2a,b. It has been reported that the complete knockout of the Slo1 gene in mice is not lethal, and mice made homozygous null for Slo1 (Slo1-KO) exhibit numerous deficits in physiological functions, which includes Slo1-KO mice whose weight increase was slower than that of wild-type littermates.[26] Another study found that there was no significant difference in the absolute weight and weight gain between the WT and Slo1-KO mice.[19] As for human, children with Slo1 mutation may tend to develop more slowly than other children.[9] In this study, we found that the body weight and size of CKO mice were not significantly different from those of

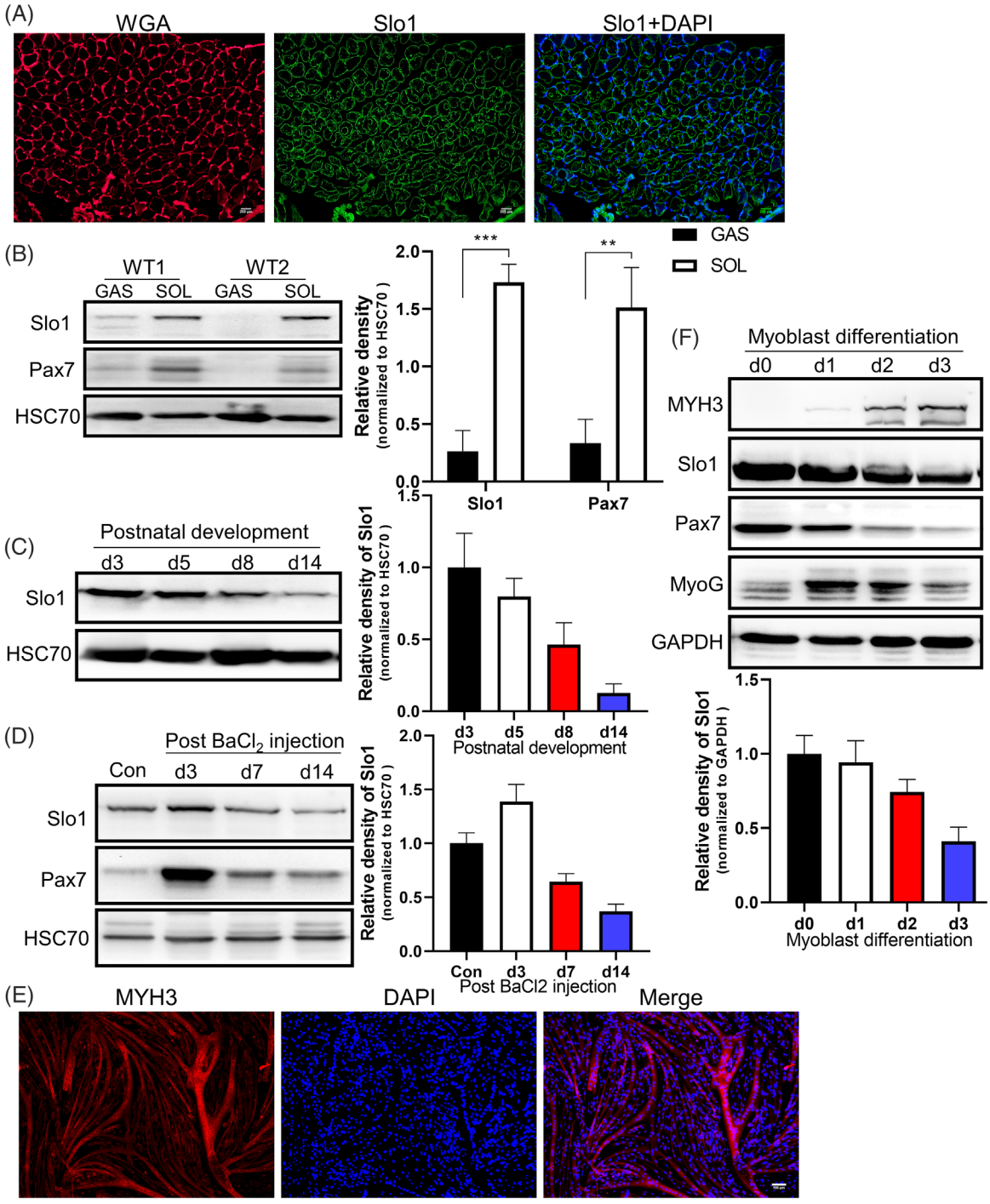

Figure 1 The expression of Slo1 in skeletal muscle and myoblasts. (A) Immunofluorescence studies revealed the expression of Slo1 in wild type (WT) soleus muscle fibre (bar = 200 μm). (B) Western blotting assays to detect Slo1 expression in various mice skeletal muscles. GAS, Gastrocnemius muscle; SOL, Soleus muscle. (C, D, F) Protein expression of Slo1 during skeletal muscle postnatal development (C), regeneration (D), and during myoblast differentiation (F). To detect Slo1 protein expression during postnatal development, as the skeletal muscles were too small to be dissected completely in newborn mice, whole calf muscle complex was collected from WT mice at postnatal days 3, 5, 8, and 14 (3 mice each group). Given that the tibialis anterior (TA) is commonly used for regeneration studies, and as a result of its superficial position, TA was used as the damaged sites in $BaCl_2$-induced injury model. TA muscles were intramuscularly injected with $BaCl_2$ and harvested 3, 7, and 14 days after injury. (E) Primary myoblasts were treated in differentiation medium for 3 days. Myotubes were stained with anti-MYH3 antibody followed by Alexa594-conjugated antibody (red) (bar = 100 μm). Results are expressed as mean ± SD (*$P < 0.05$, **$P < 0.01$, and ***$P < 0.001$).

DOI: 10.1002/jcsm.13253

WT mice in development (Figure 2A; Figure S2c) nor was the weight of the gastrocnemius muscle or soleus muscle (Figure S2d,e).

Then we performed the treadmill to test whole-body endurance. And the limb grip strength assay was used to assess muscle functions.[27] The treadmill exhaustion test indicated that the time to exhaustion covered by CKO mice was shorter than that of their control counterparts (~30% reduction, $P < 0.05$) (Figure 2B). In addition, CKO mice displayed significantly lower average grip strength than WT mice strength (~30% reduction, $P < 0.001$) (Figure 2C).

Although the function of muscles is abnormal, there is no difference in the general morphology of the muscles. Then, we examined the changes in the muscles at both the light and electron microscope levels. Myofibrillar changes were not visible under light microscopy (Figure 2D, top panel), while electron microscopy revealed a considerable reduction in the number of mitochondria in the soleus muscle

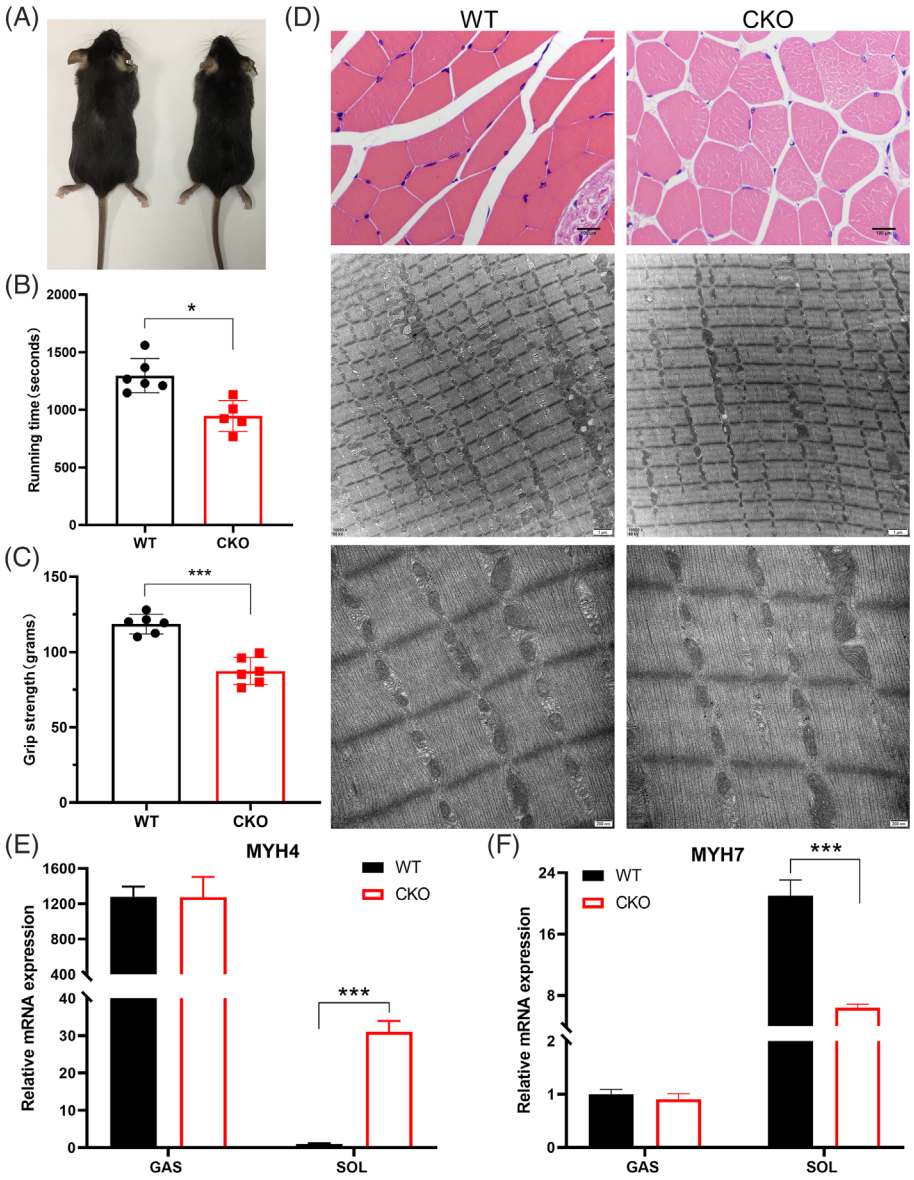

Figure 2 Slo1 deletion reduced skeletal muscle endurance and strength. (A) Gross appearance of $Slo1^{flox/flox}$ mice (WT) and $Myf5^{Cre}/Slo1^{flox/flox}$ mice (CKO). (B) Running time in seconds to exhaustion of WT ($n = 6$) and CKO ($n = 5$) mice. (C) Comparison of forelimb grip strength between CKO ($n = 6$) and WT ($n = 6$) mice. (D) Histological sections of representative muscle groups of CKO and WT mice were stained with H&E (top panel) and analysed by electron microscopy (middle and bottom panels) (bar: 100 μm, top; 1 μm, middle; 200 nm, bottom). (E, F) Expression of MYH4 (E) and MYH7 (F) transcripts in gastrocnemius (GAS) and soleus (SOL) muscle of CKO and WT mice was determined by quantitative real-time PCR ($n = 3$ in each group. mRNA expression data are normalized to GAPDH). Results are expressed as mean ± SD (*$P < 0.05$, **$P < 0.01$, and ***$P < 0.001$).

DOI: 10.1002/jcsm.13253

(Figure 2D, middle and bottom panel; ~40% reduction, $P < 0.01$, Figure S2f), similar to previous findings in muscle fibres of Slo1 mutant flies,[28] but not in the gastrocnemius muscle (Figure S2g, h).

Skeletal muscles are made up of a spectrum of different fibres, ranging from fast glycolytic type IIb fibres to slow, oxidative, fatigue-resistant type I fibres. Fibre types I exhibit an oxidative metabolism, while type IIb fibres have glycolytic capacities. Then we examined the fibre composition of the gastrocnemius (predominantly fast-twitch) and soleus (predominantly slow-twitch) muscles to elucidate the morphological and molecular underpinnings of the decreased endurance capacity of CKO mice. Interestingly, in soleus muscles of CKO mice, the mRNA level of the marker of glycolytic fibre (MYH4) was increased significantly (about 31-fold change, $P < 0.001$; Figure 2E), corresponding to the decreased MYH7 (about 3.5-fold change, $P < 0.001$; Figure 2F), which is the marker of oxidative fibre. However, this change did not occur in the gastrocnemius muscles (Figure 2E,F). These findings indicate that Slo1 may play a role in slow-twitch fibre formation.

Slo1 deletion impaired myoblast differentiation and slow-twitch fibres formation

Myotubes are developed from myoblasts and can differentiate into both slow (type I) and fast fibre types (type II). To further test the role of Slo1 in myoblast differentiation, we studied primary mouse myoblasts. After 3 days of treatment in the differentiation medium, myoblasts/CKO were able to form mature myotubes (Figure S3a), but the fusion index was significantly lower than that of myotubes derived from WT mice (myoblasts/WT) (Figure S3a, b), suggesting that Slo1 is involved in myotube formation. Consistent with the results of fusion analysis, during myoblast differentiation, the mRNA expression of myogenic marker MYH3 was lower in myoblasts/CKO than myoblasts/WT (Figure 3A). It has been reported that expression of Pax7 was confined to proliferating myoblasts and was strongly downregulated during terminal differentiation.[29] We found that Pax7 mRNA expression was not significantly reduced in the myoblasts/CKO during myoblast differentiation, compared with myoblasts/WT (Figure 3B). The corresponding protein expression levels of MYH3 and Pax7 showed similar changes (Figure 3C; Figure S3c,d). Taken together, these results demonstrate that Slo1 deletion impaired myoblast differentiation.

Given that Slo1 is primarily expressed in slow-twitch muscle fibres (Figure 1B), and MYH4 (a marker of fast-twitch fibre) mRNA expression was increased significantly in soleus muscles of CKO mice (Figure 2E,F), corresponding to the decreased MYH7 (a marker of slow-twitch fibre), it is possible that Slo1 is involved in slow-twitch fibre formation. Our results showed that MYH7 mRNA and protein expression was decreased significantly (Figure 3D,F) and MYH4 expression was increased (Figure 3E,F) during differentiation of myoblasts/CKO compared with that of myoblasts/WT. Collectively, these results suggest that Slo1 deletion can impair slow-twitch fibre formation in vivo and in vitro.

Skeletal muscle regeneration is delayed in Slo1-deficient mice

Myoblast differentiation is critical for muscle regeneration and repair after injury. To examine the function of Slo1 during skeletal muscle regeneration, we injected the tibialis anterior muscles of CKO and WT mice with $BaCl_2$ to analyse muscle regeneration after injury (Figure S1a), and assessed the expression of Desmin, which is expressed in newly formed myofibres during muscle regeneration. On day 3 after injury, the injured site had newly formed myofibres with centralized nuclei, and a mononuclear infiltration of inflammatory cells and activated myoblasts both for CKO and WT mice, but in CKO mice, the newly formed myofibres were less and smaller (more that 30% reduction in the size of regenerated muscle fibre, $P < 0.001$; Figure 4A,B), and more inflammatory cells were observed (Figure S4a). Moreover, the percentage of regenerating fibres, including two or more centralized nuclei, was significantly reduced in CKO mice (~40% reduction, $P < 0.001$), although there was no significant difference in fibre size between the two groups at 7 days after injury (Figure 4A,C).

On day 14 post injection the muscle architecture was largely restored in both CKO and WT mice, and the size of newly formed myofibres and the number of nuclei in regenerating fibres were not significantly different between the two groups by light microscopy (Figure 4A,C; Figure S4b). However, by electron microscopy we found narrow Z-discs (more that 40% reduction, $P < 0.01$; Figure 4D,E) and more glycogen granules (Figure S4c) in regenerating fibres of CKO mice, which is similar to previous findings that Z-discs were narrower and glycogen concentration was higher in fast-twitch fibres than in slow-twitch fibres.[5] In agreement with these results, we further found that MYH4 mRNA expression was increased (about 5-fold change, $P < 0.001$) while MYH7 mRNA expression decreased (about 5.7-fold change, $P < 0.001$) in CKO mice on day 14 post injection (Figure 4F). These results suggest that Slo1 deletion, to some extent, delayed skeletal muscle regeneration in the early stage of repair and impaired slow-twitch fibre formation during muscle regeneration.

Slo1 deletion influences the skeletal muscle regulation involving genes

To investigate the expression of genes involved in the muscle dysfunction induced by Slo1 deletion, RNA-seq analysis was performed in myoblasts/CKO and myoblasts/WT. Following data normalization 877 differentially expressed genes (DEGs)

DOI: 10.1002/jcsm.13253

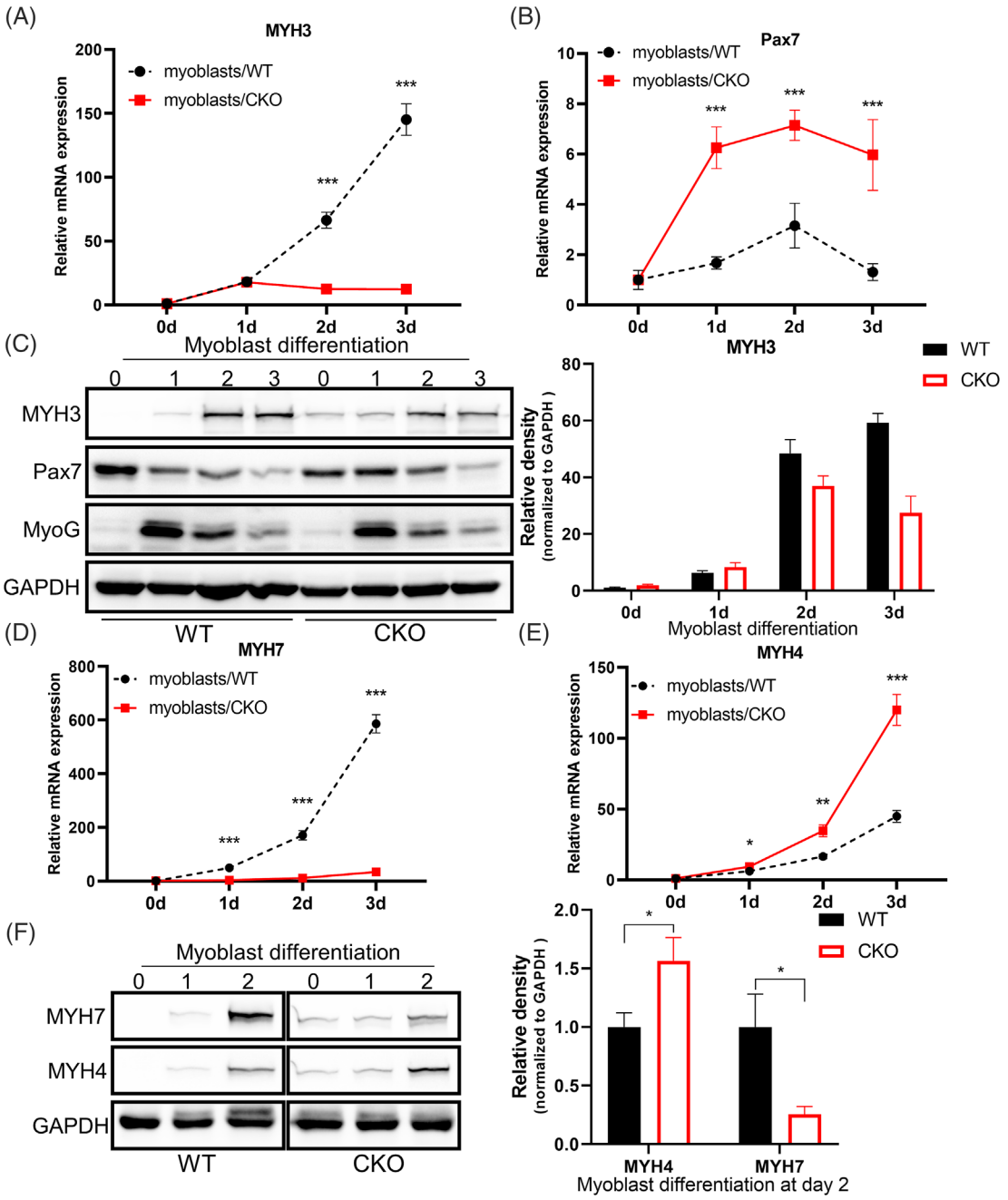

Figure 3 The expression of myogenic and fibre markers during myoblast differentiation. (A, B) Primary myoblasts derived from CKO (myoblasts/CKO) and WT (myoblasts/WT) were induced to differentiate for the indicated times. The levels of MYH3 (A) and Pax7 (B) mRNA were analysed by quantitative real-time PCR. (C) Western blotting assays to detect MYH3, Pax7 and MyoG expression during differentiation of myoblasts/CKO and myoblasts/WT. (D, E, F) MYH7 mRNA (D), MYH4 mRNA (E), and their protein (F) expression were detected for the indicated times by quantitative real-time PCR and western blotting during differentiation of myoblasts/CKO and myoblasts/WT. Results are expressed as mean ± SD (*$P < 0.05$, **$P < 0.01$, and ***$P < 0.001$).

were selected of which 553 were upregulated and 324 downregulated in myoblasts/CKO (Figure 5A; Figure S5a,b; Table S2). We found that the expression of most genes with high basal expression in skeletal muscle were downregulated in myoblasts/CKO (Table S2). Gene ontology (GO) and Kyoto Encyclopedia of Genes and Genomes (KEGG) analysis revealed that these downregulated DEGs significantly enriched in cell adhesion, cardiac muscle contraction, and vascular smooth muscle contraction; cellular component had significant enrichment in extracellular matrix and membrane-associated components (Figure 5B,C). Cell–cell communication, in which extracellular matrix and

DOI: 10.1002/jcsm.13253

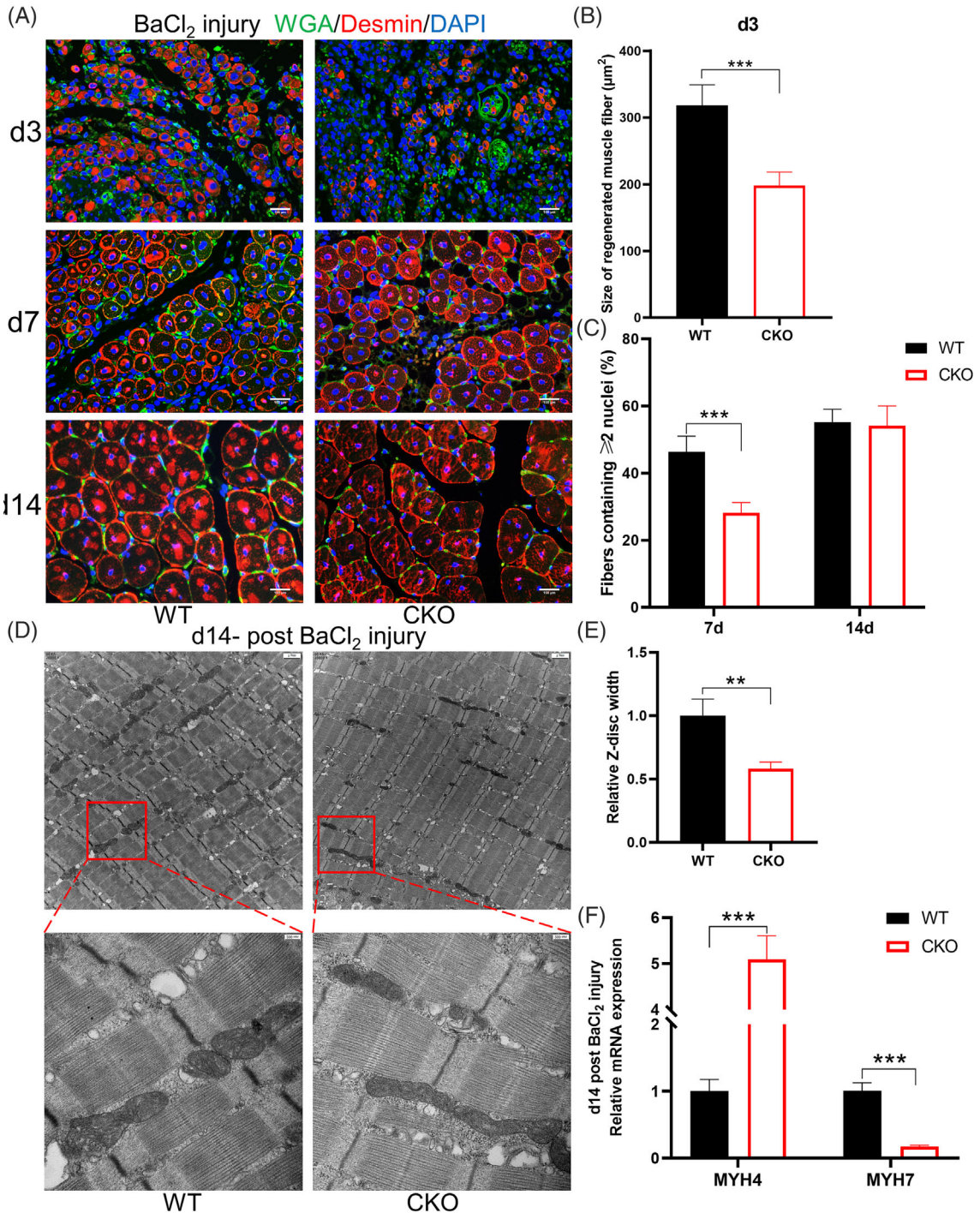

Figure 4 Skeletal muscle regeneration after injury in CKO and WT mice. (A) Regenerating tibialis anterior (TA) muscles from CKO and WT mice were stained at day 3, 7, and 14 after injury with DAPI (blue) for nuclei, Desmin (red) for newly formed myofibres, and WGA (green) for myofibre membrane boundaries (bar = 100 μm, 4 mice of each genotype were measured). (B) Fibre size were quantified at day 3 after injury in ImageJ based on Desmin (red) staining. (C) Quantification of the ratio of regenerating myofibres containing two or more centralized nuclei per field at day 7 and day 14 post injury. (D) Electron microscopy photographs of tibialis anterior muscle after 14 days muscle injury induced by $BaCl_2$ (bar = 1 μm). Red boxes are shown at higher magnification (bar = 200 nm). (E) Quantification of 100 Z-disc widths from $n = 4$ mice per group. (F) mRNA expression of MYH7 and MYH4 during WT and CKO mice muscle regeneration at day 14 after injury. Results are expressed as mean ± SD (*$P < 0.05$, **$P < 0.01$, and ***$P < 0.001$).

DOI: 10.1002/jcsm.13253

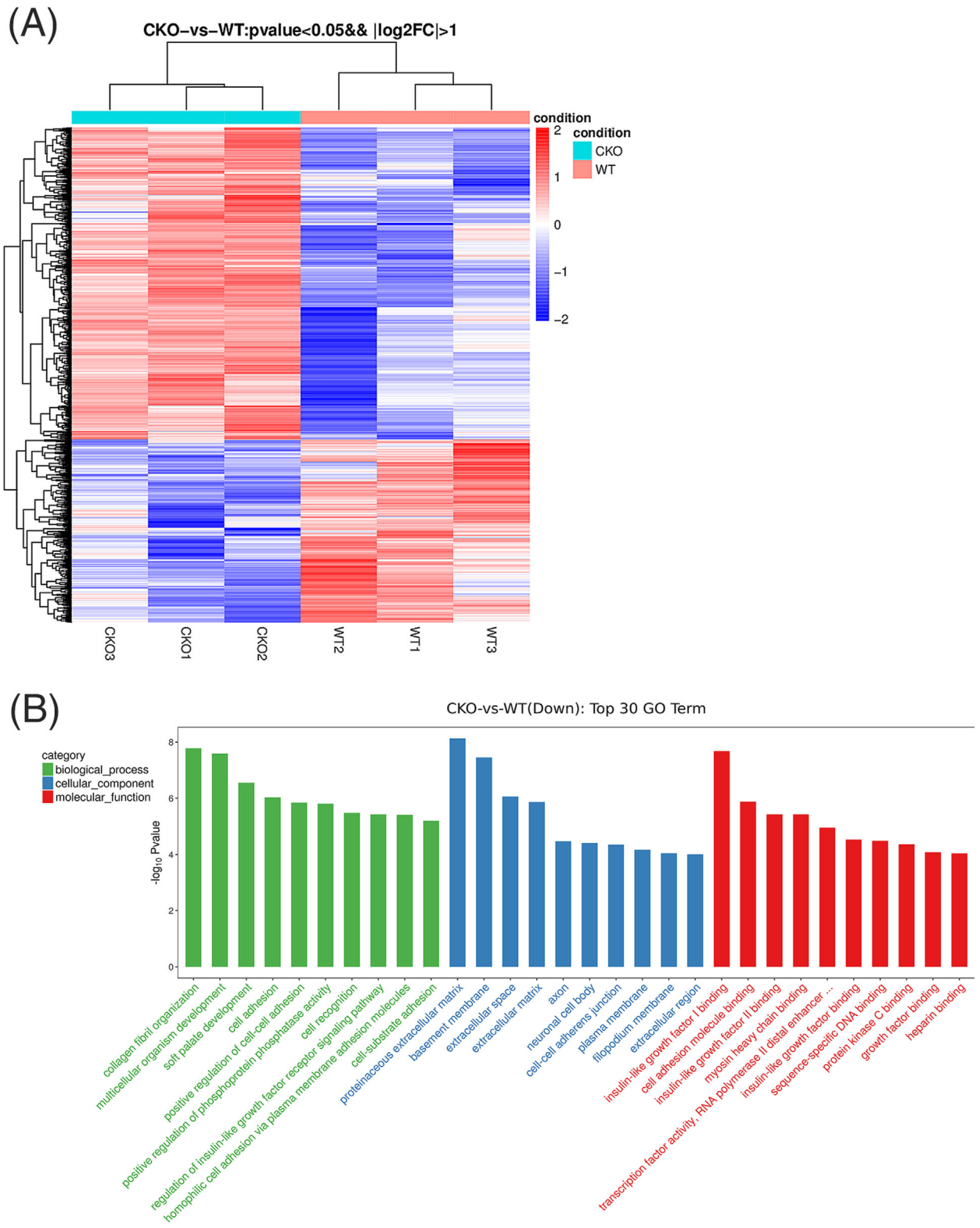

Figure 5 Differential gene expression between myoblasts/CKO and myoblasts/WT. (A) Heat map and hierarchical clustering analysis of RNA-seq data from myoblasts/CKO and myoblasts/WT based on the log 2 intensity (n = 3). (B) Gene ontology (GO) enrichment analysis of the expression of downregulated mRNAs. Representative GO terms that exhibit statistically significant differences are shown in the graphic. (C)KEGG signalling pathway enrichment of the expression of downregulated genes in myoblasts. (D, E) GSEA result of RNA-seq data of myoblasts/CKO and myoblasts/WT. Muscle contraction (D) and muscle cell differentiation (E) are enriched.

DOI: 10.1002/jcsm.13253

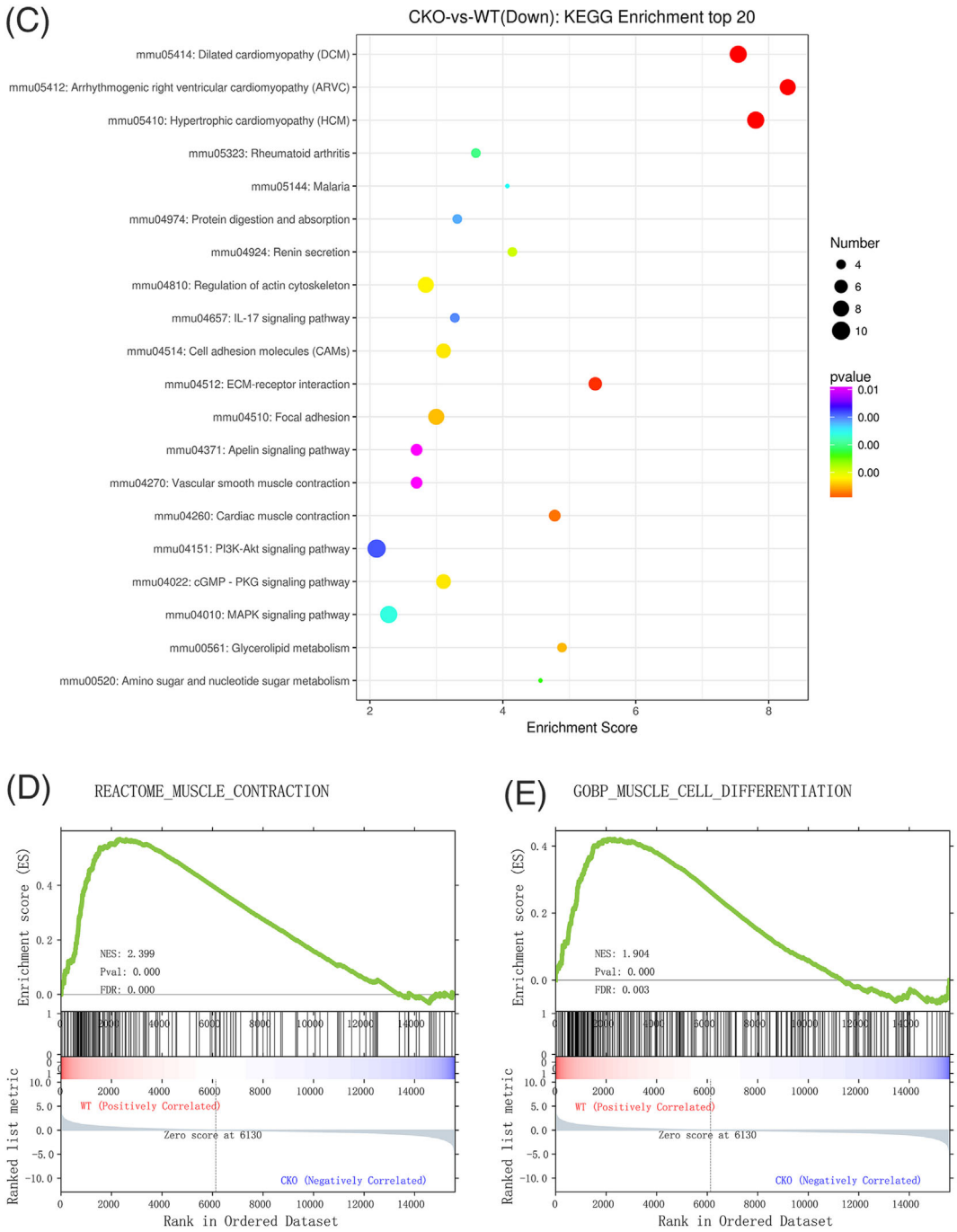

Figure 5 Continued

membrane-associated proteins play critical roles, is also important in skeletal muscle development. Cell adhesion and fusion are dependent on cell–cell communication. Furthermore, Gene Set Enrichment Analysis (GSEA) from RNA-seq analysis revealed a strong induction of muscle cell differentiation and muscle contraction genes (Figure 5D,E; Figure S5c,d). These findings might provide clues to find target genes for Slo1.

Slo1 interacts with FAK to influence myogenic differentiation

As GO and KEGG analysis revealed that DEGs were significantly involved in functions like cell adhesion and pathways like PI3K-AKT and the insulin-like growth factor receptor signalling pathway (Figure 5B,C), we focused on the factors involved in these pathways. IGF-1 promotes the differentiation

of skeletal myoblasts by activating the PI3K/Akt signalling pathway.[30] Our previous study found that Slo1 knockout impaired the activation of FAK,[13] and other research showed that Slo1 interacted with FAK in human myoblast.[31] We, therefore, hypothesized that Slo1 might be able to interact with FAK to influence the FAK-mediated PI3K-Akt pathway. To test this hypothesis, we detected the expression of FAK during myoblast differentiation, and found the protein level of FAK were downregulated (Figure 6A). Knocking down the expression of FAK with siRNA inhibited myoblast differentiation (more than 50% reduction in fusion index, $P < 0.05$; ~40% reduction in MYH3 expression, $P < 0.05$; Figure 6B–D), which is in accordance with previous findings.[32] In order to confirm the effect of Slo1 deletion on FAK-PI3K-AKT pathway, IGF-1 was used to induce myoblast differentiation. As shown in Figure 6E, Slo1 deletion reduced phosphorylation of FAK-PI3K-AKT signalling proteins in differentiating myoblasts (Figure 6E). Protein mass spectrometry was used to identify proteins in myoblasts interacted with Slo1. Unfortunately, we did not find the interaction between Slo1 and FAK from mass spectrometry results (Table S3). Then we confirmed that Slo1 binds to FAK in pri-

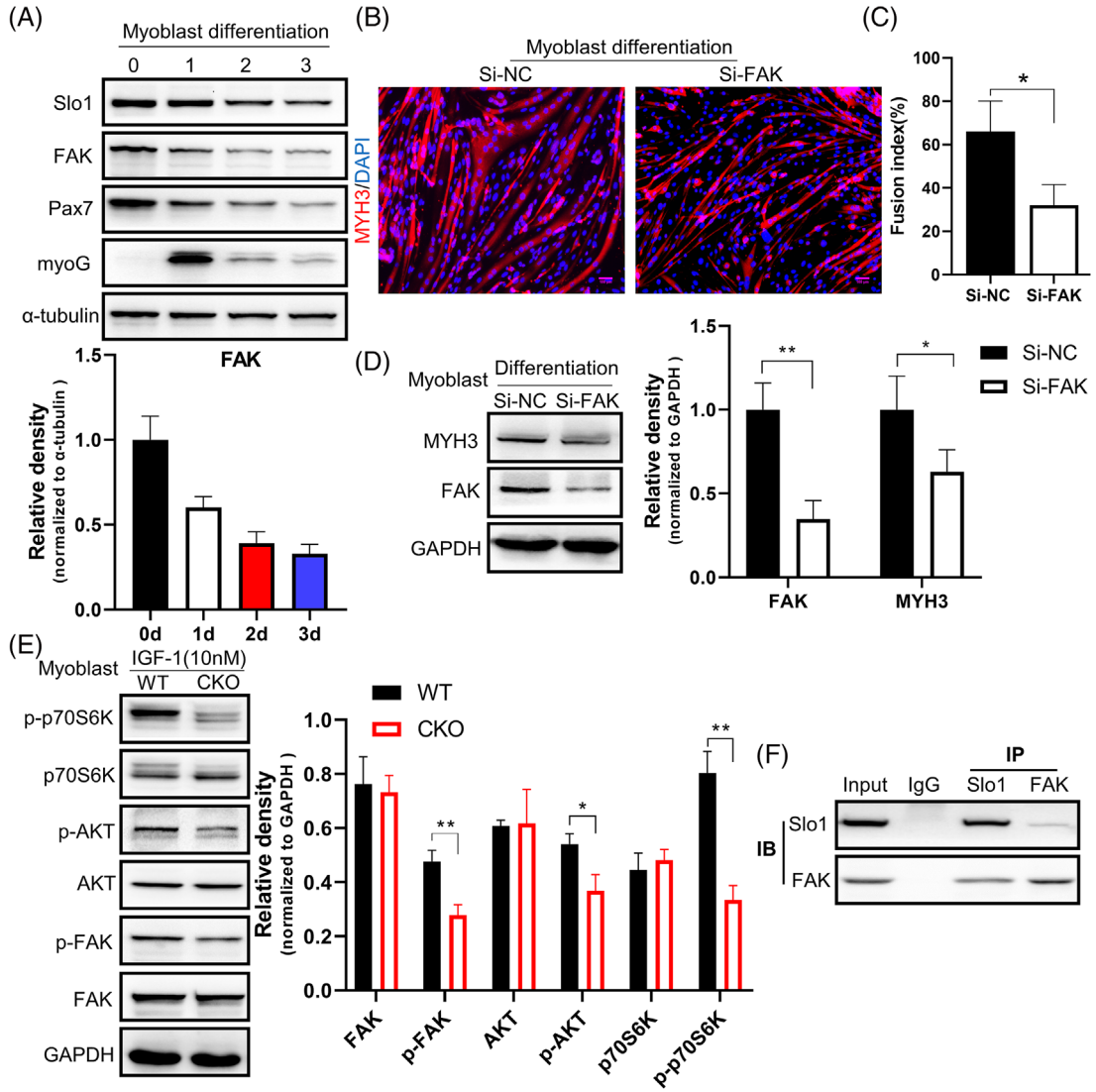

Figure 6 Slo1 interacts with FAK to regulate PI3K/AKT pathway. (A) Western blotting assays to detect the expression of FAK during myoblast differentiation. (B) Myoblasts/WT transfected with si-FAK or si-NC were induced to differentiate for 3 days then stained with a MYH3 antibody and DAPI (nuclei). (C) Fusion indices in myoblasts with knockdown of FAK were measured after 3 days of culture in differentiation medium. (D) Western blotting assays to detect MYH3 expression in myotubes developed from myoblasts with downregulated FAK. (E) Lysates of myoblasts/WT and myoblasts/CKO treated with IGF-1 (10 nM) for 15 min were western blotted with anti-pAKT (S473), p-p70S6K (Thr389), and p-FAK (Tyr397). (F) Co-immunoprecipitation (IP) of endogenous Slo1 and FAK in myoblasts. Results are expressed as mean ± SD (*$P < 0.05$, **$P < 0.01$, and ***$P < 0.001$).

DOI: 10.1002/jcsm.13253

mary mouse myoblasts by co-immunoprecipitation (Figure 6F). Collectively, these results indicate that Slo1 interacts with FAK to influence PI3K-AKT signalling during myoblast differentiation.

Slo1 deletion inhibits NFAT signalling

Calcineurin/Ca^{2+}-dependent NFAT pathway is an important regulator of slow-twitch fibre formation.[33] GSEA analysis of RNA-Seq data from myoblasts/CKO showed a significant induction of the genes regulated by NFAT pathway (P = 0.006, FDR = 0.027; Figure 7A), suggesting that Slo1 deletion impaired slow-twitch fibre formation through this pathway. In addition, GSEA analysis showed that these genes that belong to soleus muscle-associated gene set were downregulated in myoblasts/CKO, which indicated that the soleus muscle of CKO mice might have fewer slow-twitch fibre characteristics ($P < 0.001$, FDR < 0.001; Figure S6a). Furthermore, we examined the mRNA levels of troponin C1 (TNNC1) and troponin I1 (TNNI1), which are slow-twitch fibre markers, and troponin I2 (TNNI2), which is a fast-twitch fibre marker. As shown in Figure S6b, TNNC and TNNI1 were expressed at lower levels (more than 50% reduction, $P < 0.001$) in soleus muscles of CKO mice, and TNNI2 was expressed at higher levels (about 1.4-fold change, $P < 0.01$).

We found that the expression levels of NFATc2 and NFATc3 were downregulated in soleus muscles of CKO mice (~15% reduction, $P < 0.05$; Figure 7B). Consistent with this finding, significantly downregulated Rcan1 (~60% reduction, $P < 0.001$), which is specifically increased on activation of calcineurin,[34] was detected in soleus muscles of CKO mice (Figure 7C). In addition, Slo1 deletion increased the expression of key genes inhibiting NFAT activity, including Myoz1 and Myoz3, known muscle-specific inhibitors of calcineurin (Figure 7C). Furthermore, Rcan1 expression was significantly decreased during differentiation of myoblasts/CKO (Figure 7D). On the other hand, the expression of Myoz1 was significantly increased during CKO mice muscle regeneration after injury (Figure 7E). To test whether Slo1 regulates NFAT activity, we transfected primary myoblasts with Slo1 siRNA and an NFAT-luciferase reporter. Slo1 knockdown decreased luciferase activity (more than 50% reduction, $P < 0.01$, Figure 7F) in primary myoblasts, indicating that it inhibits NFAT signalling in myoblasts. Thus, Slo1 deletion diminishes slow-twitch fibre formation through the calcineurin/NFAT pathway.

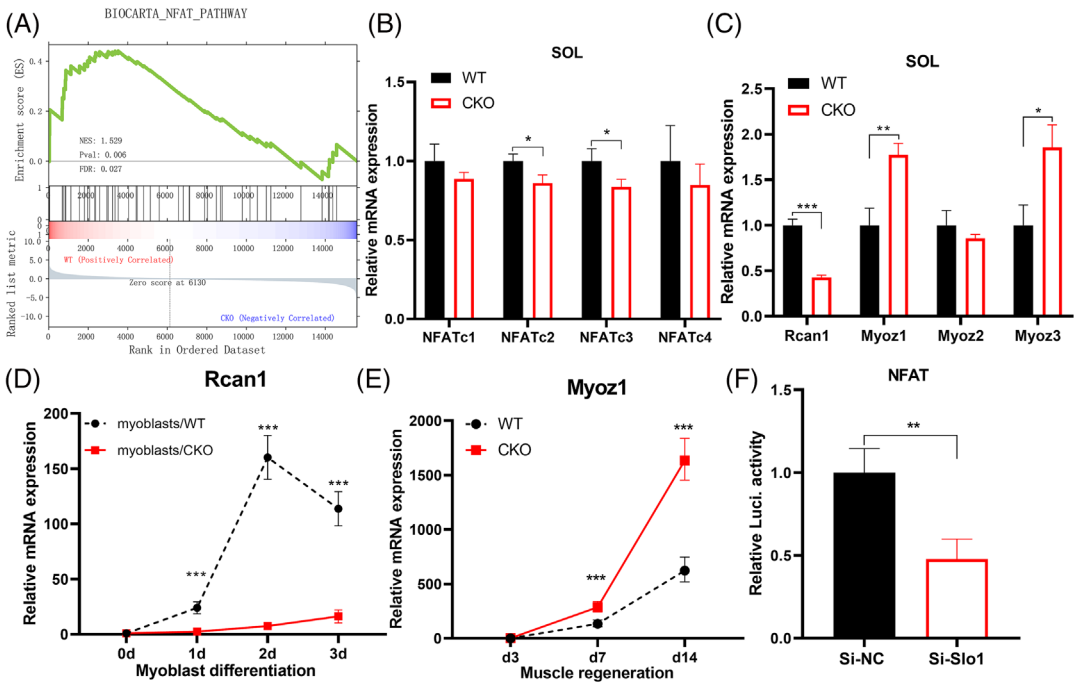

Figure 7 Slo1 deletion was associated with the expression of genes involved in NFAT signalling. (A) GSEA analysis showing that Slo1 knockout affected the expression of genes involved in calcineurin/NFAT signalling. (B) Nfatc1–4 mRNA expression in Slo1 deleted soleus muscles. (C) Effect of Slo1 deletion on the expression of genes associated with NFAT activity in soleus muscles. (D) Myoblasts were induced to differentiate for the indicated times. The level of Rcan1 mRNA was analysed by quantitative real-time PCR. (E) Myoz1 mRNA expression was analysed by quantitative real-time PCR during tibialis anterior (TA) muscle regeneration. (F) NFAT-luciferase reporter assay in myoblasts transfected with Slo1 siRNA or negative control. Results are expressed as mean ± SD (*$P < 0.05$, **$P < 0.01$, and ***$P < 0.001$).

DOI: 10.1002/jcsm.13253

Discussion

In this study, we show that Slo1 deletion in skeletal muscle dose not influence the weight of mice or the volume of muscle, slightly but significantly diminishes the grip strength. Although the treadmill test is a measure of whole-body phenotype, because of the skeletal muscle-specific knockout of Slo1, the reduced endurance of CKO mice in treadmill test is due to skeletal muscle alterations specifically. Muscle function changes in Slo1 knockout mice are more obvious and manifest as a reduced survival rate among pups.[26] Because postnatal survival demands an ability of the pup to grasp the dam, the weaker grip strength of Slo1 knockout mice might limit success at nursing. This weakness could result from impaired signal transmission at the neuromuscular junction in universal Slo1 knockout mice. In addition, the activity and muscle fibre size of $Slo1^{-/-}$ rats were decreased and tremor appeared.[17] We found that the effect of Slo1 conditional knockout on the function of skeletal muscle was not strong because the survival rate of CKO pups during the breeding process was comparable with that of WT pups (data not shown). In addition, no muscle tremors were found in CKO mice. For the rather modest loss of grip strength and endurance in the CKO mice compared with WT, some of the dysfunction observed in total Slo1 loss mice could be due to motor neuron dysfunction. Unfortunately, at present, there is no mouse model of neural system specific knockout of Slo1. Li et al. found that the locomotion speed of Slo1 deletion worms was lower than that of WT worms in early life and same Slo1 neuronal transgene failed to rescue the reduced motor activity phenotype, which indicates this phenotype in young Slo1 deletion worms may be caused by the defective muscle.[15] However, mammalian skeletal muscle is different from worm muscle, and much further work needs to be done to reveal the mechanism of Slo1 in skeletal muscle and neuron.

At the cellular level, myoblast differentiation was significantly reduced after Slo1 deletion. Because regeneration after skeletal muscle injury is closely related to the differentiation of myoblasts, we predicted that Slo1 deletion would inhibit skeletal muscle regeneration. However, the regeneration capacity of skeletal muscle in CKO mice was not significantly reduced, at least in the general structure of skeletal muscle. This may be due to the additional compensation in vivo for the effect induced by Slo1 deletion on muscle regeneration. Combining the conclusion of that study with the symptoms of the Slo1 knockout animal model, we suggest that the expression of Slo1 in skeletal muscle may not be critical for muscle development, regeneration, and performance, although it was found to inhibit myoblast differentiation in vitro.

We found that Slo1 is highly expressed in slow-twitch muscle fibres. In the process of myogenic differentiation of myoblasts with Slo1 deletion, the proportion of slow-twitch muscle fibres was significantly reduced, while the proportion of fast-twitch fibres increased. Consistent with this, in skeletal muscle regenerated after injury, the amount of newly formed slow-twitch muscle fibres decreased. Additionally, we also found that the content of mitochondria decreased and the content of glycogen increased in regenerated myofibrils of CKO mice, which is in line with the characteristics of fast-twitch muscle fibres. Previously published results reported that microgravity exposure (flown in space) induced a significant reduction in Slo1 expression and showed an expected myofibre type shift from slow to fast mainly in soleus muscle.[35] Aging is associated with a fast-to-slow fibre type shift.[36,37] A study found that an abnormally enhanced Slo1 channel current is observed during aging in fast-twitch rat muscle fibres that are undergoing a fast- to slow-twitch transition.[38] A recent study showed that genetic ablation of Slo1 on *C. elegans* motor neurons reduced the rate of age-dependent motor activity decline to slow motor aging. Interestingly, when Slo1 was manipulated early in *C. elegans* life, it had no effect on lifespan and actually had a detrimental effect on motor function. However, when Slo1 was blocked in mid-late life, both motor function and lifespan were improved.[15] We found that CKO mice display mild phenotypes in motor functions; nevertheless, older CKO mice were not examined for motor functions, nor was their lifespan in this study. Together, we speculate that the elevated expression of Slo1 may be an important cause of skeletal muscle aging.

At the molecular level, we found that deletion of Slo1 disrupts the FAK/PI3K/AKT pathway, which has been shown to control myoblast differentiation, as well as NFAT signalling, which is required and sufficient for the maintenance of the slow twitch fibre gene program. Unfortunately, our study did not delve into the further mechanisms by which Slo1 regulates NFAT signalling. It has been reported that NFATc3 deletion induced a decrease in the mRNA expression of Slo1 in murine urinary bladder smooth muscle,[39] while our findings showed that the decreased mRNA expression of NFATc3 resulted from Slo1 deletion.

In conclusion, the present results identify Slo1 as an important factor in skeletal muscle myoblast differentiation and show that Slo1 is an integral part of the slow muscle fibre program. Our results provide new directions to study and manipulate myoblast behaviour during regeneration and to better understand the role of Slo1 in muscle diseases and aging.

Acknowledgements

The present study was supported by the National Natural Science Foundation of China (82071575), the Science and Technology Commission of Shanghai Municipality (20ZR1435100,

18411964500, 16ZR1422000, and 18YF1415700), the Shanghai Municipal Health Commission (2020YJZX0122) and the Clinical Research Plan of SHDC (SHDC2020CR3086B).

The authors of this manuscript certify that they comply with the ethical guidelines for authorship and publishing in the *Journal of Cachexia, Sarcopenia and Muscle*.[40] Animal experiments of this study were approved by the Ethics Committee of Xinhua Hospital Affiliated to Shanghai Jiao Tong University School of Medicine.

Conflict of interest statement

All authors declare that they have no conflict of interest.

Online supplementary material

Additional supporting information may be found online in the Supporting Information section at the end of the article.

References

1. Schmidt M, Schuler SC, Huttner SS, von Eyss B, von Maltzahn J. Adult stem cells at work: regenerating skeletal muscle. *Cell Mol Life Sci* 2019;**76**:2559–2570.
2. Dumont NA, Wang YX, Rudnicki MA. Intrinsic and extrinsic mechanisms regulating satellite cell function. *Development* 2015;**142**:1572–1581.
3. Massenet J, Gardner E, Chazaud B, Dilworth FJ. Epigenetic regulation of satellite cell fate during skeletal muscle regeneration. *Skeletal Muscle* 2021;**11**:4.
4. Shan T, Liu J, Xu Z, Wang Y. Roles of phosphatase and tensin homolog in skeletal muscle. *J Cell Physiol* 2019;**234**:3192–3196.
5. Schiaffino S, Reggiani C. Fiber types in mammalian skeletal muscles. *Physiol Rev* 2011;**91**:1447–1531.
6. Bourdeau Julien I, Sephton CF, Dutchak PA. Metabolic Networks Influencing Skeletal Muscle Fiber Composition. *Front Cell Dev Biol* 2018;**6**:125.
7. Qaisar R, Bhaskaran S, Van Remmen H. Muscle fiber type diversification during exercise and regeneration. *Free Radic Biol Med* 2016;**98**:56–67.
8. Contreras GF, Castillo K, Enrique N, Carrasquel-Ursulaez W, Castillo JP, Milesi V, et al. A BK (Slo1) channel journey from molecule to physiology. *Channels* 2013;**7**:442–458.
9. Bailey CS, Moldenhauer HJ, Park SM, Keros S, Meredith AL. KCNMA1-linked channelopathy. *J Gen Physiol* 2019;**151**:1173–1189.
10. Niu L, Li Y, Zong P, Liu P, Shui Y, Chen B, et al. Melatonin promotes sleep by activating the BK channel in C elegans. *Proc Natl Acad Sci U S A* 2020;**117**:25128–25137.
11. Sancho M, Kyle BD. The Large-Conductance, Calcium-Activated Potassium Channel: A Big Key Regulator of Cell Physiology. *Front Physiol* 2021;**12**:750615.
12. Toro L, Li M, Zhang Z, Singh H, Wu Y, Stefani E. MaxiK channel and cell signalling. *Pflugers Archiv: Eur J Physiol* 2014;**466**:875–886.
13. Wang Y, Guo Q, Hei H, Tao J, Zhou Y, Dong J, et al. BK ablation attenuates osteoblast bone formation via integrin pathway. *Cell Death Dis* 2019;**10**:738.
14. Abraham LS, Oh HJ, Sancar F, Richmond JE, Kim H. An alpha-catulin homologue controls neuromuscular function through localization of the dystrophin complex and BK channels in Caenorhabditis elegans. *PLoS Genet* 2010;**6**:e1001077.
15. Li G, Gong J, Liu J, Liu J, Li H, Hsu AL, et al. Genetic and pharmacological interventions in the aging motor nervous system slow motor aging and extend life span in C. elegans. *Sci Adv* 2019;**5**:eaau5041.
16. Meredith AL, Thorneloe KS, Werner ME, Nelson MT, Aldrich RW. Overactive bladder and incontinence in the absence of the BK large conductance Ca2+−activated K+ channel. *J Biol Chem* 2004;**279**:36746–36752.
17. He C, Li X, Wang M, Zhang S, Liu H. Deletion of BK channels decreased skeletal and cardiac muscle function but increased smooth muscle contraction in rats. *Biochem Biophys Res Commun* 2021;**570**:8–14.
18. Maqoud F, Cetrone M, Mele A, Tricarico D. Molecular structure and function of big calcium-activated potassium channels in skeletal muscle: pharmacological perspectives. *Physiol Genomics* 2017;**49**:306–317.
19. Typlt M, Mirkowski M, Azzopardi E, Ruettiger L, Ruth P, Schmid S. Mice with deficient BK channel function show impaired prepulse inhibition and spatial learning, but normal working and spatial reference memory. *PLoS ONE* 2013;**8**:e81270.
20. Tajhya RB, Hu X, Tanner MR, Huq R, Kongchan N, Neilson JR, et al. Functional KCa1.1 channels are crucial for regulating the proliferation, migration and differentiation of human primary skeletal myoblasts. *Cell Death Dis* 2016;**7**:e2426.
21. Kim JB, Kim SJ, Kang SY, Yi JW, Kim SM. The large-conductance calcium-activated potassium channel holds the key to the conundrum of familial hypokalemic periodic paralysis. *Korean J Pediatr* 2014;**57**:445–450.
22. Jiang L, Yang Q, Gao J, Yang J, He J, Xin H, et al. BK Channel Deficiency in Osteoblasts Reduces Bone Formation via the Wnt/beta-Catenin Pathway. *Mol Cells* 2021;**44**:557–568.
23. Hindi L, McMillan JD, Afroze D, Hindi SM, Kumar A. Isolation, Culturing, and Differentiation of Primary Myoblasts from Skeletal Muscle of Adult Mice. *Bioanalysis* 2017;**7**:7.
24. Xia C, Jiang T, Wang Y, Chen X, Hu Y, Gao Y. The p53/miR-145a Axis Promotes Cellular Senescence and Inhibits Osteogenic Differentiation by Targeting Cbfb in Mesenchymal Stem Cells. *Front Endocrinol* 2020;**11**:609186.
25. Tricarico D, Mele A, Conte CD. Phenotype-dependent functional and pharmacological properties of BK channels in skeletal muscle: effects of microgravity. *Neurobiol Dis* 2005;**20**:296–302.
26. Halm ST, Bottomley MA, Almutairi MM, Di Fulvio M, Halm DR. Survival and growth of C57BL/6J mice lacking the BK channel, Kcnma1: lower adult body weight occurs together with higher body fat. *Physiol Rep* 2017;**5**:5.
27. Castro B, Kuang S. Evaluation of Muscle Performance in Mice by Treadmill Exhaustion Test and Whole-limb Grip Strength Assay. *Bio-protocol* 2017;**7**:7.
28. Gururaja Rao S, Bednarczyk P, Towheed A, Shah K, Karekar P, Ponnalagu D, et al. BKCa (Slo) Channel Regulates Mitochondrial Function and Lifespan in Drosophila melanogaster. *Cell* 2019;**8**:945.
29. Halevy O, Piestun Y, Allouh MZ, Rosser BW, Rinkevich Y, Reshef R, et al. Pattern of Pax7 expression during myogenesis in the posthatch chicken establishes a model for satellite cell differentiation and renewal. *Dev Dynam* 2004;**231**:489–502.
30. Glass DJ. PI3 kinase regulation of skeletal muscle hypertrophy and atrophy. *Curr Top Microbiol Immunol* 2010;**346**:267–278.
31. Rezzonico R, Cayatte C, Bourget-Ponzio I, Romey G, Belhacene N, Loubat A, et al. Focal adhesion kinase pp125FAK interacts with the large conductance calcium-activated hSlo potassium channel in human osteoblasts: potential role in mechanotransduction. *J Bone Min Res* 2003;**18**:1863–1871.
32. Lee HJ, Kao CY, Lin SC, Xu M, Xie X, Tsai SY, et al. Dysregulation of nuclear receptor COUP-TFII impairs skeletal muscle development. *Sci Rep* 2017;**7**:3136.
33. Bassel-Duby R, Olson EN. Signaling pathways in skeletal muscle remodeling. *Annu Rev Biochem* 2006;**75**:19–37.

34. Kingsbury TJ, Cunningham KW. A conserved family of calcineurin regulators. *Genes Dev* 2000;**14**:1595–1604.
35. Gambara G, Salanova M, Ciciliot S, Furlan S, Gutsmann M, Schiffl G, et al. Gene Expression Profiling in Slow-Type Calf Soleus Muscle of 30 Days Space-Flown Mice. *PLoS ONE* 2017;**12**:e0169314.
36. Larsson L, Karlsson J. Isometric and dynamic endurance as a function of age and skeletal muscle characteristics. *Acta Physiol Scand* 1978;**104**:129–136.
37. Miljkovic N, Lim JY, Miljkovic I, Frontera WR. Aging of skeletal muscle fibers. *Ann Rehabil Med* 2015;**39**:155–162.
38. Tricarico D, Petruzzi R, Camerino DC. Changes of the biophysical properties of calcium-activated potassium channels of rat skeletal muscle fibres during aging. *Pflugers Archiv: Eur J Physiol* 1997;**434**:822–829.
39. Layne JJ, Werner ME, Hill-Eubanks DC, Nelson MT. NFATc3 regulates BK channel function in murine urinary bladder smooth muscle. *Am J Physiol Cell Physiol* 2008;**295**: C611–C623.
40. von Haehling S, Morley JE, Coats AJ, Anker SD. Ethical guidelines for publishing in the Journal of Cachexia, Sarcopenia and Muscle: update 2021. *J Cachexia Sarcopenia Muscle* 2021;**12**:2259–2261.